Chemical Science

ROYAL SOCIETY OF CHEMISTRY

EDGE ARTICLE

View Article Online
View Journal | View Issue

Cite this: *Chem. Sci.*, 2025, **16**, 18911

All publication charges for this article have been paid for by the Royal Society of Chemistry

Received 27th June 2025
Accepted 6th September 2025

DOI: 10.1039/d5sc04751j

rsc.li/chemical-science

Simple, one-step syntheses of tri- and tetracyclic B,N,S-heterocycles from reactions of a diboracumulene with thiols

Christian Markl,[ab] Sourav Kar,[ab] Lukas Lubczyk,[ab] Kai Hammond,[ab] Rian D. Dewhurst[ab] and Holger Braunschweig[*ab]

Boron-containing fused heterocycles have received considerable attention due to their unique structures, bonding, and intriguing properties. However, progress in this area has been hampered by a lack of efficient synthetic methodologies. In this study, we demonstrate the reactivity of a diboracumulene, LBBL (L = cyclic (alkyl)(amino)carbene, CAAC), with various nitrogen-containing heterocyclic thiols. These straightforward reactions result in the partial or complete cleavage of the B–B multiple bonds in the diboracumulene, along with S–H bond activation in the thiol units, leading to the formation of a range of tricyclic and tetracyclic B,N,S-heterocycles. Notably, the tricyclic B,N,S-heterocycle exhibits π aromaticity in all three of its rings.

Introduction

Fused heterocyclic compounds are common structural motifs found in natural products, pharmaceuticals, and functional materials, and they have garnered significant attention in recent years.[1–7] In particular, nitrogen-containing fused heterocycles play a crucial role in the development of various drugs, pesticides, and functional materials.[2,3,5–7] Notably, the incorporation of electron-deficient boron atoms into these fused heterocycles has led to the discovery of a wide range of unique compounds (Fig. 1A), owing to boron's ability to modulate the energies and distributions of frontier molecular orbitals and their ability to interact with biologically-relevant molecules.[8–19] For example, boron-containing heterocyclic drugs such as tavaborole (**I**) and crisaborole have been approved by the United States FDA, while many others are currently undergoing clinical trials.[8] Boron-doped heterocycles **II–IV** display distinctive photophysical and optoelectronic properties (Fig. 1A).[9–11] Despite these promising applications, existing synthetic methods for constructing boron-based fused heterocycles remain limited, primarily relying on boron-doping *via* salts or small-molecule elimination, or metallacycle transfer.[20–26] Also, these methodologies are mostly restricted to the use of B_1-containing reagents (Fig. 1B). However, Liu and coworkers recently demonstrated that the cycloaddition reaction between bis-diazidoborane and isonitriles can yield boron-containing tricyclic heterocycles.[27] Further, we showed that the insertion of azides into the B–B single bond of cyclic diboranes results in the formation of novel B,N-heterocycles.[28] In light of the increasing interest in boron-containing heterocycles, efforts have intensified to identify unique diboron-based synthons and to develop innovative strategies for their incorporation into the synthesis of fused heterocycles.

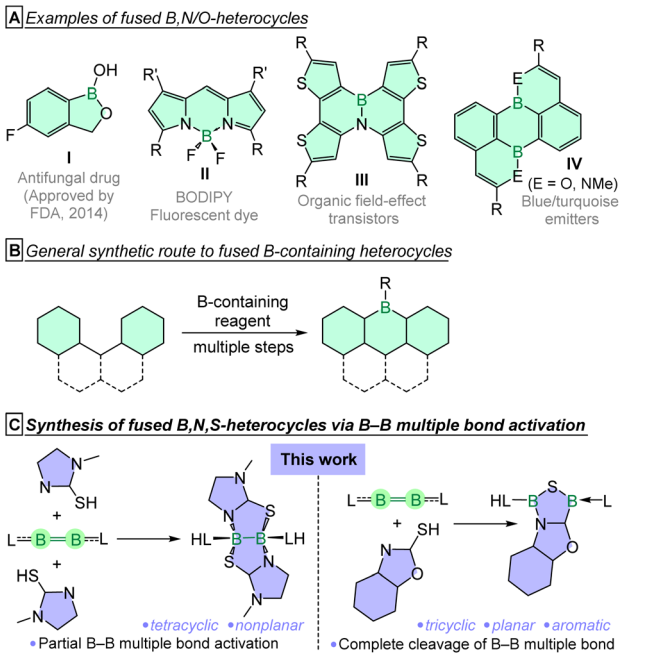

Fig. 1 (A) Examples of fused B,N/O-heterocycles. (B) General synthetic route to fused B-containing heterocycles. (C) Synthesis of fused B,N,S-heterocycles *via* B–B multiple bond activation (this work). (L = CAAC).

[a]*Institute for Inorganic Chemistry, Julius-Maximilians-Universität Würzburg, Am Hubland, 97074 Würzburg, Germany. E-mail: h.braunschweig@uni-wuerzburg.de*
[b]*Institute for Sustainable Chemistry & Catalysis with Boron, Julius-Maximilians-Universität Würzburg, Am Hubland, 97074 Würzburg, Germany*

In this context, the highly reactive diboracumulene $[B_2(CAAC)_2]$ (**1**),[29] featuring electron-rich B–B and B–C(CAAC) multiple bonding, exhibits a broad and versatile reactivity profile.[30–41] Notably, B_2L_2 (L = CAAC or NHC)[29,42] species featuring B–B multiple bonds exhibit a wide range of intermolecular bond activation reactions *via* 1,2-addition mechanisms, including the activation of H–H,[33] B–H,[36] C–H,[39,40] B–B,[37] C–O,[34,35] S–S,[38] and Se–Se[38] bonds. Thus, diboracumulene **1** was seen as a promising diboron source for the synthesis of boron-based fused heterocycles. Recently, we have shown that the reaction of diboracumulene **1** with pyridine yielded a tricyclic diazadiborinine derivative.[43] On the other hand, the S–H bond has proven to be highly reactive. N-containing heterocyclic thiols, which possess such reactive S–H units, are well-suited for 1,2-addition reactions involving both nitrogen and sulfur centres following S–H activation.[44] Thus, the combination of diboracumulene **1** with various N-containing heterocyclic thiols offers a potential strategy for constructing fused B,N,S-heterocycles. Herein, we report the synthesis of various tricyclic and tetracyclic B,N,S-heterocycles *via* S–H bond activation, accompanied by partial or complete cleavage of the B–B multiple bonds.

Results and discussion

The room-temperature reaction of diboracumulene **1** with two equivalents of 1-phenyl-1*H*-tetrazole-5-thiol in benzene led to a colour change from purple to colourless (Scheme 1). The ^{11}B NMR spectrum of the resulting colourless reaction mixture showed a new chemical shift at δ = 10.0 ppm, significantly upfield from that of diboracumulene **1** (δ = 80.0 ppm). After workup, a colourless solid (**2**) was isolated in 75% yield. A single-crystal X-ray diffraction (SCXRD) analysis revealed **2** to comprise a tetracyclic B,N,S-heterocycle, resulting from the S–H activation of two thiol groups and their symmetrical coordination to the B_2 unit from both sides through nitrogen and sulfur centres in a μ_2,η^2 binding mode (Fig. 2 (left)). The tetracyclic **2** is formed by the fusion of two planar five-membered CN_4 rings and two envelope-shaped five-membered CB_2NS rings. The

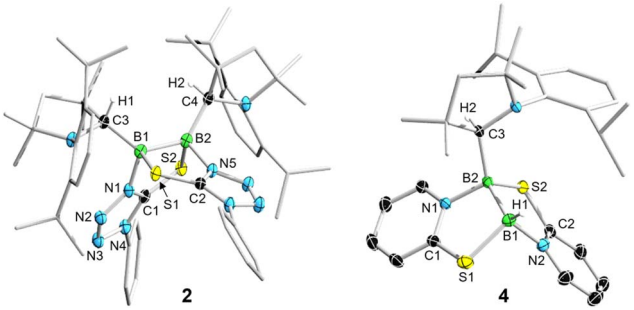

Fig. 2 Crystallographically-determined molecular structures of **2** (left) and **4** (right). Ellipsoids are shown at the 50% probability level. All hydrogen atoms and ellipsoids of the ligand periphery are omitted for clarity. Selected bond lengths of **2** (in Å): B1–B2 1.846(6), B1–S1 2.032(5), B2–S2 2.017(8), B1–N1 1.594(6), B2–N5 1.590(5), B1–C3 1.639(7), and B2–C4 1.649 (5). Selected bond lengths of **4** (in Å): B1–B2 1.733(2), B1–S1 1.954(1), B2–S2 1.980(1), B1–N2 1.599(2), B2–N1 1.622(1), and B2–C3 1.637(2).

hydrogen atoms from the S–H units migrate to the CAAC ligands upon activation (H1 and H2, Fig. 2 (left)), which is also evident from a singlet ^1H NMR signal at δ = 4.40 ppm, consistent with reported chemical shifts for protonated CAAC units.[43,45,46] Notably, the B–B bond (1.846(6) Å) in **2** is significantly longer than the B–B multiple bond (1.489(2) Å) in **1** (ref. 29) and falls in the expected range of B–B single bond of diboranes.[30,31,47,48] The B1–C3 (1.639(7) Å) and B2–C4 (1.649 (5) Å) bond distances in **2** also indicate single covalent character. The fusion of two N-containing heterocyclic thiol units across the B–B bond in **2** leads to a nearly eclipsed conformation with a *cis* arrangement of (H–CAAC)–B–B–(CAAC–H) moiety. The small S1–B1–B2–N5 (22.9(1)°) and S2–B2–B1–N1 (22.6(1)°) dihedral angles reflect the rigidity of the fused tetracyclic system. The N–B distances (N1–B1: 1.594(6) Å; N5–B2: 1.590(5) Å) fall within the range typical for dative N→B bonds,[44,49] whereas the S–B distances (S1–B1: 2.032(5) Å; S2–B2: 2.017(8) Å) indicate single covalent bonds. Thus, the fused tetracyclic heterocycle **2** can also be interpreted as a doubly base-stabilised, symmetrical cyclic diborane(4).

Further, we have carried out the room-temperature reaction of diboracumulene **1** with another five-membered heterocyclic thiol, namely 1-methyl-1*H*-imidazole-2-thiol (2 equivalents) in benzene, which also led to the isolation of a colourless solid **3** in 77% yield (Scheme 1). The ^{11}B NMR spectrum of **3** showed a signal at δ = 15.1 ppm, slightly downfield of that of tetracyclic **2** (δ = 10.0 ppm). Also, the ^1H NMR spectrum of **3** displayed a pattern similar to that of tetracyclic **2**. For example, a singlet ^1H NMR signal at δ = 4.19 ppm was observed for **3**, which is slightly upfield relative to the peak at δ = 4.40 ppm corresponding to the migrated hydrogens from S–H to the CAAC ligands in tetracyclic **2**. These findings suggest the formation of an analogue of **2**. Indeed, a SCXRD analysis confirmed **3** as a tetracyclic B,N,S-heterocycle, in which four five-membered rings are fused (Fig. S21). However, due to disorder, the structural parameters of **3** cannot be discussed in detail.

To investigate the effect of heterocyclic thiol ring size on the formation of fused heterocycles, diboracumulene **1** was treated

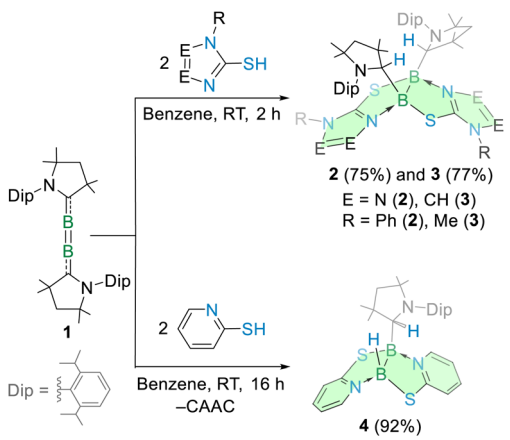

Scheme 1 Synthesis of tetracyclic B,N,S-heterocycles **2**–**4**.

with a six-membered heterocyclic thiol, namely pyridine-2-thiol (2 equivalents). After 16 hours, the reaction led to the isolation of a colourless solid **4** in 92% yield (Scheme 1). Unlike the symmetrical tetracyclic B,N,S-heterocycles **2** and **3**, the ^{11}B NMR spectrum of **4** exhibited two distinct signals at δ = 10.8 and 0.8 ppm. In line with the ^{11}B NMR spectrum, the SCXRD study of **4** showed an unsymmetrical tetracyclic B,N,S-heterocyclic species (Fig. 2 (right)). Although the core geometry of **4** is composed of four fused rings similar to tetracyclic **2** and **3**, it differs by consisting of two six-membered and two five-membered rings. The dissymmetry in tetracyclic **4** arises from the presence of one B–H unit and one B–(CAAC–H) unit, rather than two B–(CAAC–H) units as found in **2** and **3**. This also suggests that one of the CAAC ligands of diboracumulene **1** is substituted by a hydrogen atom transferred from the S–H group of pyridine-2-thiol to form **4**. The presence of a terminal B–H unit in fused **4** is further confirmed by the ^{1}H{^{11}B} NMR signal at δ = 4.45 ppm and the IR stretching band observed at 2465 cm^{-1}. Meanwhile, the other hydrogen from a second S–H group migrates to the carbene carbon of the second CAAC ligand, facilitating the formation of compound **4**. The B–B bond length in **4** (1.733(2) Å) is significantly shorter than that in fused **2**, though it still falls within the typical range for B–B single bonds in diboranes.[30,31,47,48] The S–B distances in tetracyclic **4** (S1–B1: 1.954(1) Å; S2–B2: 1.980(1) Å) are also slightly shorter than those observed in tetracyclic **2**. In contrast, the B2–C3 (1.637(2) Å) and N–B (N2–B1: 1.599(2) Å; N1–B2: 1.622(1) Å) distances of tetracyclic **4** are comparable to those in **2**, indicating covalent B–C and dative N→B single bonds, respectively. Similar to tetracyclic **2**, the fusion of two N-containing six-membered heterocyclic thiol moieties across the B–B bond in **4** results in a nearly eclipsed structure, featuring a *cis* arrangement of (H–CAAC)–B–B–(H). Notably, the dihedral angles S1–B1–B2–N1 (10.4(1)°) and S2–B2–B1–N2 (5.9(1)°) in tetracyclic **4** are considerably smaller than those in **2**, suggesting a more rigid fused tetracyclic framework in **4**.

Although no intermediates were detected for tetracyclic **2** and **3**, the reactions likely proceed *via* initial adduct formation between the diboracumulene and two thiol units at the nitrogen center, followed by rapid 1,2 S–H addition to both B–C_{CAAC} units (Scheme S1). In the case of tetracyclic **4**, initial adduct formation is also expected; however, the use of a six-membered thiol introduces steric repulsion between the CAAC and the pyridine derivative. This rapidly results in the simultaneous dissociation of one CAAC ligand, 1,1 S–H addition at the exposed boron center, and 1,2 S–H addition at the other B–C_{CAAC} unit, leading to the formation of **4** (Scheme S1).

Having prepared a series of tetracyclic B,N,S-heterocycles **2–4**, we carried out density functional theory (DFT) calculations at the ωB97X-D/Def2-SVP level of theory to gain insight into their structure and bonding. The B–B bond in optimised **4** (1.737 Å) is shorter than those of fused **2** (1.848 Å) and **3** (1.854 Å), possibly due to reduced steric crowding resulting from the smaller substituent at B1 in the former. Nonetheless, all three B–B bond lengths fall within the typical range for B–B single bonds, which is also evident from the Wiberg bond indices (WBIs) of the B–B bonds in **2–4** (Table 1). On the other hand, the natural population analysis of **4** showed a lower natural charge on the boron atom bearing a hydrogen substituent (q_{B1} = 0.01) than the other boron atom (q_{B2} = 0.39), suggesting comparatively higher electron density at B1. This polarisation in the B–B bond in **4** is also reflected in the experimental (δ = 0.8 and 10.8 ppm) and calculated (δ = 2.2 (B1) and 11.5 (B2) ppm) ^{11}B NMR spectra. Also, the calculated ^{11}B NMR chemical shifts for fused **2** (δ = 11.7 ppm) and **3** (δ = 11.9 ppm) are in good agreement with the experimental values (δ = 10.0 and 15.1 ppm, respectively). Further, the highest occupied molecular orbitals (HOMOs) of fused **2** and **3** mainly correspond to the σ-bonding interactions through the H–C_{CAAC}–B–B–C_{CAAC}–H unit (Fig. 3), while the HOMO–4 of fused **4** depicts σ-bonding interactions in the S–B–B–S and B–H units (Fig. 3).

We subsequently turned to bicyclic thiol systems to investigate whether steric effects influence the formation of fused rings. The room-temperature reaction of diboracumulene **1** with two equivalents of benzo[*d*]thiazole-2-thiol in benzene afforded a colourless solid **5** in 75% yield (Fig. 4). The ^{11}B NMR spectrum of **5** exhibited two distinct chemical shifts at δ = 50.3 and −10.8 ppm, indicating a significant difference of 61 ppm. This large disparity suggests that the two boron atoms reside in markedly different electronic environments.

A SCXRD analysis revealed that compound **5** adopts a tetracyclic B,N,S-heterocyclic core structure, but one that completely differs from those of tetracyclic B,N,S-heterocycles **2–4**. The core tetracyclic geometry of **5** is composed of one five-membered and three six-membered rings (Fig. 4 (inset)). Following S–H activation, one of the thiol heterocycles participates in fused-ring

Table 1 Experimental and calculated bond lengths (d), WBIs, natural charges at boron (q_B) and ^{11}B NMR chemical shifts of fused **2–4**[a]

	B–B			B–N			B–S					
	Exp. d [Å]	Calc. d [Å]	WBI	Exp. d [Å]	Calc. d [Å]	WBI	Exp. d [Å]	Calc. d [Å]	WBI	q_B	Exp. ^{11}B NMR [ppm]	Cal. ^{11}B NMR [ppm]
2	1.846 (6)	1.848	0.91	1.594 (6)	1.594	0.87	2.032 (5)	2.020	0.94	0.41	10.0	11.7
				1.590 (5)	1.594	0.87	2.017 (8)	2.020	0.94			
3	*a*	1.854	0.91	*a*	1.590	0.87	*a*	2.021	0.94	0.42	15.1	11.9
4	1.733 (2)	1.737	0.96	1.622 (1)	1.622	0.82	1.980 (1)	1.981	1.01	0.39 (B2)	10.8 (B2)	11.5 (B2)
				1.599 (2)	1.597	0.85	1.954 (1)	1.956	1.05	0.01 (B1)	0.8 (B1)	2.2 (B1)

[a] Due to disorder, the structural parameters of **3** cannot be discussed.

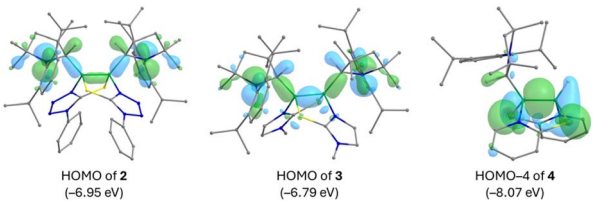

Fig. 3 Selected frontier molecular orbitals of fused tetracyclic compounds **2**–**4** (isovalue 0.043 a.u.).

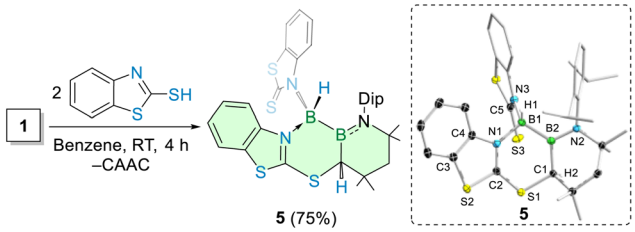

Fig. 4 Synthesis of tetracyclic B,N,S-heterocycle **5**. Inset: crystallographically-determined molecular structure of **5** (ellipsoids shown at the 50% probability level). All hydrogen atoms and ellipsoids of ligand periphery are omitted for clarity. Selected bond lengths of **5** (in Å): B1–B2 1.715(2), B1–N1 1.609(2), B1–N3 1.585(2), C1–S1 1.823(2), B2–N2 1.414(2), B2–C1 1.599(2), and C5–S3 1.669(1).

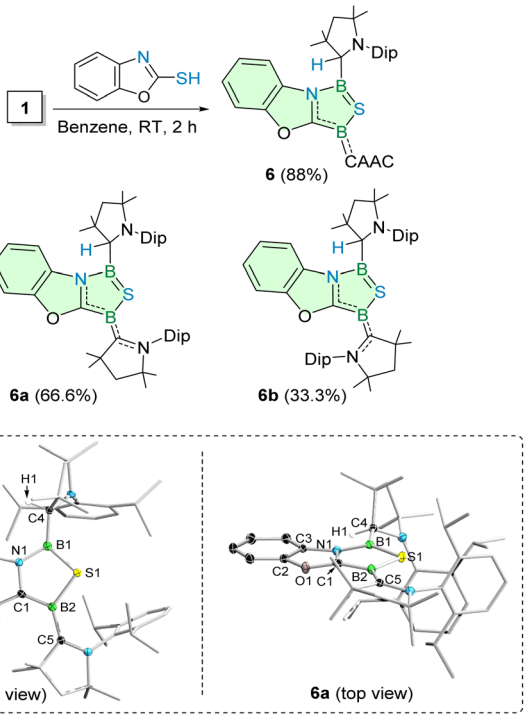

Fig. 5 Synthesis of tricyclic B,N,S-heterocycle **6** and representation and ratio of the two rotamers of **6** observed by NMR spectroscopy. Inset: crystallographically-determined molecular structure of **6a**; front view (left), top view (right). Ellipsoids shown at the 50% probability level. All hydrogen atoms and ellipsoids of ligand periphery are omitted for clarity. Selected bond lengths of **6a** (in Å): B1–N1 1.461(1), B2–C1 1.485(2), B1–S1 1.791(1), B2–S1 1.880(1), C1–N1 1.395(2), C3–N1 1.410(2) Å, C1–O1 1.384(1), and C2–O1 1.379(2).

formation with the B_2 unit and the ring-expanded CAAC moiety, while the other functions as a substituent at one of the boron centres (B1). The B–B bond length in **5** (1.715(2) Å) is shorter than those observed in fused **2** and **4**, yet still falls within the expected range for B–B single bonds.[30,31,47,48] Furthermore, the WBI value of 0.96 for the B–B bond in **5** confirms the presence of a single bond. One of these boron atoms (B1) is tetracoordinate, while the other boron atom (B2) is tricoordinate—consistent with the upfield ($\delta = -10.8$ ppm) and downfield ($\delta =$ 50.3 ppm) ^{11}B NMR signals, respectively. These assignments are further supported by DFT-calculated ^{11}B NMR chemical shifts at $\delta = -12.4$ (B1) and 49.9 ppm (B2), which closely match the experimental values. The distinction between the two boron centres is also reflected in their natural charges ($q_{B1} = 0.19$ and $q_{B2} = 0.78$).

In contrast, the reaction of diboracumulene **1** with a different bicyclic thiol, benzo[*d*]oxazole-2-thiol, yielded the yellow solid **6** in 88% yield. The ^{11}B NMR spectrum of **6** showed two chemical shifts at $\delta = 41.8$ and 6.4 ppm, like tetracyclic **5**, indicating two distinct chemical environments for the boron atoms. However, the complex ^{1}H NMR spectrum of **6** revealed the presence of two rotational isomers **6a** and **6b** in a 2 : 1 ratio. An SCXRD analysis revealed a tricyclic core structure comprising one six-membered ring and two five-membered rings (Fig. 5). The formation of the fused tricyclic core involves complete cleavage of the B=B double bond in **1**, followed by insertion of a sulfur atom, originating from the thiol unit, between the two boron atoms. The remaining fragment of the bicyclic thiol bonded to the B_2 fragment from the opposite side, resulting in the observed fused tricyclic architecture. One of the boron centres (B1) is covalently single-bonded to the CAACH unit (B1–C4: 1.584(2) Å), while the other boron atom (B2) is partially double-bonded to the CAAC unit (B2–C5: 1.506(2) Å), which is also evident from WBI, MO, and NLMO analyses (Fig. 6, S29 and S30). Note that the molecular structure shown in Fig. 5 (inset) corresponds to isomer **6a**, which is identified as the major isomer by ^{1}H NMR spectroscopy. Rotation of the CAAC ligand by 180° yields isomer **6b** (Fig. 5 and S31), which is only 1.48 kcal mol^{-1} higher in energy than the major isomer **6a** (Gibbs free energies calculated at 298 K).

Interestingly, all three rings of the tricyclic framework in **6a** are coplanar, as shown in Fig. 5 (top view). Moreover, the B–N (1.461(1) Å), B–C (1.485(2) Å), B–S (1.791(1) and 1.880(1) Å), C–N (1.395(2) and 1.410(2) Å), C–O (1.379(2) and 1.384(1) Å), and C–C (1.379(2)–1.397(2) Å) bond distances within the tricyclic framework of **6a** are comparable to those reported for corresponding partial double bonds, indicating extended delocalization.[43,50,51] Also, the calculated bond distances and WBIs support the partial double bonding in the tricyclic core of **6a** (Fig. 6A). We performed adaptive natural density partitioning (AdNDP)[52,53] analysis, which revealed 144 localized orbitals containing 288 valence electrons. These were distributed into three lone pairs, 254 σ-bonding electrons (2c–2e), and 28 π-bonding electrons. Of the π-bonding electrons, 16 participate in delocalized multicenter–two-electron (mc–2e) π-bonding interactions spanning all three rings of the tricyclic framework (Fig. 6B).

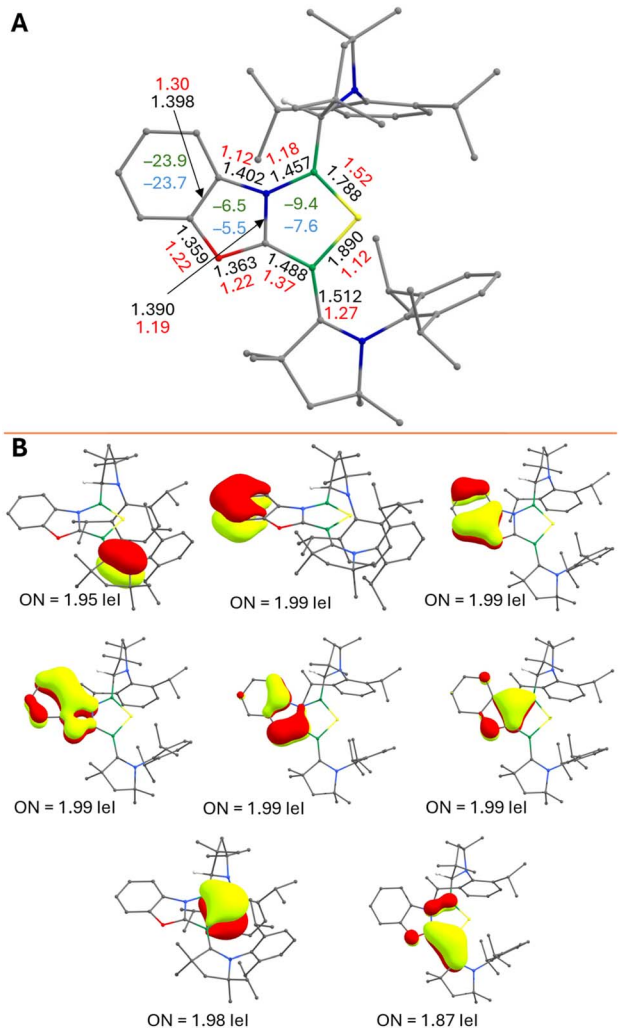

Fig. 6 (A) Optimised geometry of **6a**. Interatomic distances (in Å), WBIs, NICS(1)$_{zz}$ and NICS(−1)$_{zz}$ are given in black, red, green and sky blue, respectively. (B) Selected π bonding interactions of **6a**, obtained from AdNDP analysis. The occupancy threshold of 1.8 is used for the selection of candidate localized orbitals. Hydrogens omitted for clarity (isovalue 0.043 a.u.).

Furthermore, the natural localized molecular orbital (NLMO) analysis of fused **6a** supported the presence of these delocalized π-bonding interactions (Fig. S30). All these bond parameters and bonding interactions suggested the aromaticity of the coplanar tricyclic rings in **6a**, which prompted us to perform nucleus-independent chemical shift (NICS) analysis.[54] The NICS$_{zz}$ values 1 Å above (NICS(1)$_{zz}$) and below (NICS(−1)$_{zz}$) the six-membered ring are more negative than those of both five-membered rings in fused **6a** (Fig. 6A), indicating greater π aromaticity in the six-membered ring. Nevertheless, the significantly negative NICS(1)$_{zz}$ and NICS(−1)$_{zz}$ values for all three rings support the classification of the entire tricyclic core of **6a** as π aromatic.

To identify the absorption responsible for the yellow color of tricyclic **6**, we recorded its UV-vis spectrum, which showed a band at λ = 460 nm (Fig. S17). Time-dependent DFT calculations (Table S2 and Fig. S32) attribute this absorption to a HOMO→LUMO transition, primarily involving excitation of $\pi_{(C1-B2-C5)}$ electrons to the corresponding π* orbitals.

Despite differing only by the heteroatom (S or O), the two thiol substrates exhibited markedly different reactivities, yielding tetracyclic **5** and tricyclic **6**. Benzo[*d*]oxazole-2-thiol is more prone to losing its terminal sulfur atom (SH group) than benzo[*d*]thiazole-2-thiol. This difference primarily arises from the differing electronegativities of the heteroatoms (S *vs.* O) in their respective ring systems. Oxygen, being more electronegative than sulfur, withdraws electron density from the terminal SH group, thereby weakening the adjacent C–S bond in benzo[*d*]oxazole-2-thiol and making it more susceptible to cleavage. As a result, terminal C–S bond cleavage was observed in benzo[*d*]oxazole-2-thiol, leading to the formation of tricyclic **6**. In contrast, benzo[*d*]thiazole-2-thiol underwent only S–H or N–H bond activation (associated with thione–thiol tautomerism), resulting in the formation of tetracyclic **5**. Notably, the reaction of the diboracumulene with one equivalent of benzo[*d*]thiazole-2-thiol resulted in only partial formation of tetracyclic **5**; full conversion required two equivalents of benzo[*d*]thiazole-2-thiol. Another likely factor is the higher aromaticity of benzo[*d*]thiazole-2-thiol compared to benzo[*d*]oxazole-2-thiol, due to greater π-electron delocalization in the former. In pursuit of increased aromatic stabilization, benzo[*d*]oxazole-2-thiol favours the formation of an aromatic tricyclic framework **6**.

Conclusions

In summary, a series of fused B,N,S-heterocycles, comprising either four- or three-ring systems, was synthesised. These complex and novel fused heterocycles were synthesised from simple one-pot reactions between a diboracumlene and various heterocyclic thiols *via* B–B multiple bond and S–H bond activations. Monocyclic thiols produced symmetrical, butterfly-shaped tetracyclic cores, while bicyclic thiols yielded an unsymmetrical tetracyclic core and an aromatic tricyclic framework. Given the growing interest in boron-based polyheterocycles, this synthetic approach represents a significant advancement and is expected to accelerate the discovery of novel fused heterocycles.

Author contributions

Supervision, funding acquisition, conceptualization: H. B.; conceptualization, formal analysis, investigation: C. M.; investigation, formal analysis, visualization, writing – original draft: S. K.; formal analysis: L. L.; investigation: K. H.; writing – review & editing: R. D. D.

Conflicts of interest

There are no conflicts to declare.

Data availability

CCDC 2467669, 2467670, 2467671, 2467672 and 2467673 contain the supplementary crystallographic data for this paper.[55a–e]

The data supporting this article have been included as part of the SI. Supplementary information: Synthetic, spectroscopic, X-ray crystallographic and computational details. See DOI: https://doi.org/10.1039/d5sc04751j.

Acknowledgements

Financial support from the Deutsche Forschungsgemeinschaft is gratefully acknowledged (466954611). S. K. thanks the Alexander von Humboldt Foundation for a postdoctoral fellowship.

Notes and references

1 C. Zheng and S.-L. You, Catalytic asymmetric dearomatization (CADA) reaction-enabled total synthesis of indole-based natural products, *Nat. Prod. Rep.*, 2019, **36**, 1589–1605.
2 E. Vitaku, D. T. Smith and J. T. Njardarson, Analysis of the Structural Diversity, Substitution Patterns, and Frequency of Nitrogen Heterocycles among U.S. FDA Approved Pharmaceuticals, *J. Med. Chem.*, 2014, **57**, 10257–10274.
3 R. D. Taylor, M. MacCoss and A. D. G. Lawson, Rings in Drugs, *J. Med. Chem.*, 2014, **57**, 5845–5859.
4 L. D. Lavis and R. T. Raines, Bright Ideas for Chemical Biology, *ACS Chem. Biol.*, 2008, **3**, 142–155.
5 D. Ye, H. Lu, Y. He, Z. Zheng, J. Wu and H. Wei, Rapid syntheses of N-fused heterocycles *via* acyl-transfer in heteroaryl ketones, *Nat. Commun.*, 2022, **13**, 3337.
6 L. Ding, Z.-D. Yu, X.-Y. Wang, Z.-F. Yao, Y. Lu, C.-Y. Yang, J.-Y. Wang and J. Pei, Polymer Semiconductors: Synthesis, Processing, and Applications, *Chem. Rev.*, 2023, **123**, 7421–7497.
7 H. Gao, Q. Zhang and J. M. Shreeve, Fused heterocycle-based energetic materials (2012–2019), *J. Mater. Chem. A*, 2020, **8**, 4193–4216.
8 B. C. Das, M. A. Shareef, S. Das, N. K. Nandwana, Y. Das, M. Saito and L. M. Weiss, Boron-Containing heterocycles as promising pharmacological agents, *Bioorg. Med. Chem.*, 2022, **63**, 116748.
9 G. Ulrich, R. Ziessel and A. Harriman, The Chemistry of Fluorescent Bodipy Dyes: Versatility Unsurpassed, *Angew. Chem., Int. Ed.*, 2008, **47**, 1184–1201.
10 X.-Y. Wang, H.-R. Lin, T. Lei, D.-C. Yang, F.-D. Zhuang, J.-Y. Wang, S.-C. Yuan and J. Pei, Azaborine Compounds for Organic Field-Effect Transistors: Efficient Synthesis, Remarkable Stability, and BN Dipole Interactions, *Angew. Chem., Int. Ed.*, 2013, **52**, 3117–3120.
11 T. Kaehler, M. Bolte, H.-W. Lerner and M. Wagner, Introducing Perylene as a New Member to the Azaborine Family, *Angew. Chem., Int. Ed.*, 2019, **58**, 11379–11384.
12 K. Zhao, Z.-F. Yao, Z.-Y. Wang, J.-C. Zeng, L. Ding, M. Xiong, J.-Y. Wang and J. Pei, "Spine Surgery" of Perylene Diimides with Covalent B–N Bonds toward Electron-Deficient BN-Embedded Polycyclic Aromatic Hydrocarbons, *J. Am. Chem. Soc.*, 2022, **144**, 3091–3098.
13 Z. X. Giustra and S.-Y. Liu, The State of the Art in Azaborine Chemistry: New Synthetic Methods and Applications, *J. Am. Chem. Soc.*, 2018, **140**, 1184–1194.
14 D. E. Bean and P. W. Fowler, Effect on Ring Current of the Kekulé Vibration in Aromatic and Antiaromatic Rings, *J. Phys. Chem. A*, 2011, **115**, 13649–13656.
15 A. Wakamiya, T. Taniguchi and S. Yamaguchi, Intramolecular B–N Coordination as a Scaffold for Electron-Transporting Materials: Synthesis and Properties of Boryl-Substituted Thienylthiazoles, *Angew. Chem., Int. Ed.*, 2006, **45**, 3170–3173.
16 K. Liu, R. A. Lalancette and F. Jäkle, B–N Lewis Pair Functionalization of Anthracene: Structural Dynamics, Optoelectronic Properties, and O_2 Sensitization, *J. Am. Chem. Soc.*, 2017, **139**, 18170–18173.
17 X. Long, Z. Ding, C. Dou, J. Zhang, J. Liu and L. Wang, Polymer Acceptor Based on Double B←N Bridged Bipyridine (BNBP) Unit for High-Efficiency All-Polymer Solar Cells, *Adv. Mater.*, 2016, **28**, 6504–6508.
18 C. Dou, X. Long, Z. Ding, Z. Xie, J. Liu and L. Wang, An Electron-Deficient Building Block Based on the B←N Unit: An Electron Acceptor for All-Polymer Solar Cells, *Angew. Chem., Int. Ed.*, 2016, **55**, 1436–1440.
19 R. J. Grams, W. L. Santos, I. R. Scorei, A. Abad-García, C. A. Rosenblum, A. Bita, H. Cerecetto, C. Viñas and M. A. Soriano-Ursúa, The Rise of Boron-Containing Compounds: Advancements in Synthesis, Medicinal Chemistry, and Emerging Pharmacology, *Chem. Rev.*, 2024, **124**, 2441–2511.
20 P. A. Chase, W. E. Piers and B. O. Patrick, New Fluorinated 9-Borafluorene Lewis Acids, *J. Am. Chem. Soc.*, 2000, **122**, 12911–12912.
21 T. Hatakeyama, S. Hashimoto, S. Seki and M. Nakamura, Synthesis of BN-Fused Polycyclic Aromatics *via* Tandem Intramolecular Electrophilic Arene Borylation, *J. Am. Chem. Soc.*, 2011, **133**, 18614–18617.
22 D. R. Levine, M. A. Siegler and J. D. Tovar, Thiophene-Fused Borepins As Directly Functionalizable Boron-Containing π-Electron Systems, *J. Am. Chem. Soc.*, 2014, **136**, 7132–7139.
23 J. Radtke, K. Schickedanz, M. Bamberg, L. Menduti, D. Schollmeyer, M. Bolte, H.-W. Lerner and M. Wagner, Selective access to either a doubly boron-doped tetrabenzopentacene or an oxadiborepin from the same precursor, *Chem. Sci.*, 2019, **10**, 9017–9027.
24 C. R. McConnell and S.-Y. Liu, Late-stage functionalization of BN-heterocycles, *Chem. Soc. Rev.*, 2019, **48**, 3436–3453.
25 K. E. Krantz, S. L. Weisflog, N. C. Frey, W. Yang, D. A. Dickie, C. E. Webster and R. J. Gilliard, Planar, Stair-stepped, and Twisted: Modulating Structure and Photophysics in Pyrene- and Benzene-Fused N-Heterocyclic Boranes, *Chem.–Eur. J.*, 2020, **26**, 10072–10082.
26 M. Crumbach, J. Bachmann, L. Fritze, A. Helbig, I. Krummenacher, H. Braunschweig and H. Helten, Dithiophene-Fused Oxadiborepins and Azadiborepins: A

New Class of Highly Fluorescent Heteroaromatics, *Angew. Chem., Int. Ed.*, 2021, **60**, 9290–9295.
27 T.-T. Liu and Y.-S. Cui, One-Pot Access to Boron-Doped Fused Heterocycles *via* Domino Cyclization of Bis-Diazidoboranes with Isonitrile, *Chem.–Eur. J.*, 2023, **29**, e202302683.
28 D. Prieschl, M. Arrowsmith, M. Dietz, A. Rempel, M. Müller and H. Braunschweig, *Chem. Commun.*, 2020, **56**, 5681–5684.
29 J. Böhnke, H. Braunschweig, W. C. Ewing, C. Hörl, T. Kramer, I. Kummenacher, J. Mies and A. Vargas, Diborabutatriene: An Electron-Deficient Cumulene, *Angew. Chem., Int. Ed.*, 2014, **53**, 9082–9085.
30 M. Arrowsmith, H. Braunschweig and T. E. Stennett, Formation and Reactivity of Electron-Precise B–B Single and Multiple Bonds, *Angew. Chem., Int. Ed.*, 2017, **56**, 96–115.
31 H. Braunschweig and R. D. Dewhurst, Single, Double, Triple Bonds and Chains: The Formation of Electron-Precise B–B Bonds, *Angew. Chem., Int. Ed.*, 2013, **52**, 3574–3583.
32 J. Böhnke, H. Braunschweig, P. Constantinidis, T. Dellermann, W. C. Ewing, I. Fischer, K. Hammond, F. Hupp, J. Mies, H.-C. Schmitt and A. Vargas, Experimental Assessment of the Strengths of B–B Triple Bonds, *J. Am. Chem. Soc.*, 2015, **137**, 1766–1769.
33 M. Arrowsmith, J. Böhnke, H. Braunschweig, M. A. Celik, T. Dellermann and K. Hammond, Uncatalyzed Hydrogenation of First-Row Main Group Multiple Bonds, *Chem.–Eur. J.*, 2016, **22**, 17169–17172.
34 M. Arrowsmith, J. Böhnke, H. Braunschweig and M. A. Celik, Reactivity of a Dihydrodiborene with CO: Coordination, Insertion, Cleavage, and Spontaneous Formation of a Cyclic Alkyne, *Angew. Chem., Int. Ed.*, 2017, **56**, 14287–14292.
35 A. Stoy, J. Böhnke, J. O. C. Jimenéz-Halla, R. D. Dewhurst, T. Thiess and H. Braunschweig, CO_2 Binding and Splitting by Boron–Boron Multiple Bonds, *Angew. Chem., Int. Ed.*, 2018, **57**, 5947–5951.
36 T. Brückner, T. E. Stennett, M. Heß and H. Braunschweig, Single and Double Hydroboration of B–B Triple Bonds and Convergent Routes to a Cationic Tetraborane, *J. Am. Chem. Soc.*, 2019, **141**, 14898–14903.
37 T. Brückner, R. D. Dewhurst, T. Dellermann, M. Müller and H. Braunschweig, Mild synthesis of diboryldiborenes by diboration of B–B triple bonds, *Chem. Sci.*, 2019, **10**, 7375–7378.
38 J. Böhnke, T. Dellermann, M. A. Celik, I. Krummenacher, R. D. Dewhurst, S. Demeshko, W. C. Ewing, K. Hammond, M. Heß, E. Bill, E. Welz, M. Röhr, R. Mitrić, B. Engels, F. Meyer and H. Braunschweig, Isolation of diborenes and their 90°-twisted diradical congeners, *Nat. Commun.*, 2018, **9**, 1197.
39 J. Böhnke, T. Brückner, A. Hermann, O. F. González-Belman, M. Arrowsmith, J. O. C. Jiménez-Halla and H. Braunschweig, Single and double activation of acetone by isolobal B≡N and B≡B triple bonds, *Chem. Sci.*, 2018, **9**, 5354–5359.
40 T. Brückner, M. Arrowsmith, M. Heß, K. Hammond, M. Müller and H. Braunschweig, Synthesis of fused B,N-heterocycles by alkyne cleavage, NHC ring-expansion and C–H activation at a diboryne, *Chem. Commun.*, 2019, **55**, 6700–6703.
41 M. Arrowsmith, J. Böhnke, H. Braunschweig, M. A. Celik, C. Claes, W. C. Ewing, I. Krummenacher, K. Lubitz and C. Schneider, Neutral Diboron Analogues of Archetypal Aromatic Species by Spontaneous Cycloaddition, *Angew. Chem., Int. Ed.*, 2016, **55**, 11271–11275.
42 H. Braunschweig, R. D. Dewhurst, K. Hammond, J. Mies, K. Radacki and A. Vargas, Ambient-Temperature Isolation of a Compound with a Boron-Boron Triple Bond, *Science*, 2012, **336**, 1420–1422.
43 T. Brückner, B. Ritschel, J. O. C. Jiménez-Halla, F. Fantuzzi, D. Duwe, C. Markl, R. D. Dewhurst, M. Dietz and H. Braunschweig, Metal-Free Intermolecular C–H Borylation of N-Heterocycles at B–B Multiple Bonds, *Angew. Chem., Int. Ed.*, 2023, **62**, e202213284.
44 A. Ahmad, S. Gayen, S. Mishra, Z. Afsan, S. Bontemps and S. Ghosh, Doubly Base-Stabilised Diborane(4) and Borato-Boronium Species and Their Chemistry with Chalcogens, *Inorg. Chem.*, 2024, **63**, 3376–3382.
45 D. Auerhammer, M. Arrowsmith, H. Braunschweig, R. D. Dewhurst, J. O. C. Jimenez-Halla and T. Kupfer, Nucleophilic addition and substitution at coordinatively saturated boron by facile 1,2-hydrogen shuttling onto a carbene donor, *Chem. Sci.*, 2017, **8**, 7066–7071.
46 G. D. Frey, J. D. Masuda, B. Donnadieu and G. Bertrand, Activation of Si–H, B–H, and P–H Bonds at a Single Nonmetal Center, *Angew. Chem., Int. Ed.*, 2010, **49**, 9444–9447.
47 R. Borthakur, K. Saha, S. Kar and S. Ghosh, Recent advances in transition metal diborane(6), diborane(4) and diborene(2) chemistry, *Coord. Chem. Rev.*, 2019, **399**, 213021.
48 H.-J. Himmel, Boron-Boron Single Bonds Mimicking Transition Metals, *Eur. J. Inorg. Chem.*, 2025, **28**, e202500214.
49 T. Trageser, D. Bebej, M. Bolte, H.-W. Lerner and M. Wagner, B–B *vs.* B–H Bond Activation in a (μ-Hydrido)diborane(4) Anion upon Cycloaddition with CO_2, Isocyanates, or Carbodiimides, *Angew. Chem., Int. Ed.*, 2021, **60**, 13500–13506.
50 Y. Su, Y. Li, R. Ganguly and R. Kinjo, Engineering the Frontier Orbitals of a Diazadiborinine for Facile Activation of H_2, NH_3, and an Isonitrile, *Angew. Chem., Int. Ed.*, 2018, **57**, 7846–7849.
51 M. Weber, T. Kupfer, M. Arrowsmith, R. D. Dewhurst, M. Rang, B. Ritschel, S. Titlbach, M. Ernst, M. O. Rodrigues, E. N. da Silva Júnior and H. Braunschweig, Bypassing Ammonia: From N_2 to Nitrogen Heterocycles without N_1 Intermediates or Transition Metals, *Angew. Chem., Int. Ed.*, 2024, **63**, e202402777.
52 D. Y. Zubarev and A. I. Boldyrev, Developing paradigms of chemical bonding: adaptive natural density partitioning, *Phys. Chem. Chem. Phys.*, 2008, **10**, 5207–5217.
53 N. V. Tkachenko and A. I. Boldyrev, Chemical bonding analysis of excited states using the adaptive natural density partitioning method, *Phys. Chem. Chem. Phys.*, 2019, **21**, 9590–9596.

54 H. Fallah-Bagher-Shaidaei, C. S. Wannere, C. Corminboeuf, R. Puchta and P. v. R. Schleyer, Which NICS Aromaticity Index for Planar π Rings Is Best?, *Org. Lett.*, 2006, **8**, 863–866.

55 (*a*) C. Markl S. Kar L. Lubczyk K. Hammond R. D. Dewhurst and H. Braunschweig, CCDC 2467669: Experimental Crystal Structure Determination, 2025, DOI: **10.5517/ccdc.csd.cc2ntt7k**; (*b*) C. Markl S. Kar L. Lubczyk K. Hammond R. D. Dewhurst and H. Braunschweig, CCDC 2467670: Experimental Crystal Structure Determination, 2025, DOI: **10.5517/ccdc.csd.cc2ntt8l**; (*c*) C. Markl S. Kar L. Lubczyk K. Hammond R. D. Dewhurst and H. Braunschweig, CCDC 2467671: Experimental Crystal Structure Determination, 2025, DOI: **10.5517/ccdc.csd.cc2ntt9m**; (*d*) C. Markl S. Kar L. Lubczyk K. Hammond R. D. Dewhurst and H. Braunschweig, CCDC 2467672: Experimental Crystal Structure Determination, 2025, DOI: **10.5517/ccdc.csd.cc2nttbn**; (*e*) C. Markl S. Kar L. Lubczyk K. Hammond R. D. Dewhurst and H. Braunschweig, CCDC 2467673: Experimental Crystal Structure Determination, 2025, DOI: **10.5517/ccdc.csd.cc2nttcp**.